Title

Interferon-β induction heterogeneity during KSHV infection is determined by interferon-β enhanceosome transcription factors other than IRF3

Authors

Machika Kaku[*, †] and Marta Maria Gaglia[†]

Footnote

[*]Program in Immunology, Tufts Graduate School of Biomedical Sciences, Boston, MA

[†]Department of Medical Microbiology and Immunology, Institute for Molecular Virology, and Carbone Cancer Center, University of Wisconsin - Madison, WI

ORCIDs: 0000-0002-9921-0678 (M.K.); 0000-0002-1791-0663 (M.M.G.)

Address correspondence and reprint requests to Dr. Marta Gaglia, University of Wisconsin-Madison, 1525 Linden Dr, Madison, WI 53706. E-mail address: marta.gaglia@wisc.edu. Phone number: (608)263-5551

This work was supported by National Institutes of Health Grant R01 CA268976 to M.M.G. and by the University of Wisconsin-Madison, Office of the Vice Chancellor for Research and Graduate Education with funding from the Wisconsin Alumni Research Foundation. The UWCCC Flow Cytometry Laboratory is supported by the UWCCC Cancer Center Grant P30 CA014520.

Abbreviations used in this article: A549, lung carcinoma cell line; ATF2, activating transcription factor 2; BC-3, KSHV-infected B cell line isolated from a patient with primary effusion lymphoma; BJAB, KSHV-negative B cell lymphoma line; casp-i, pan caspase inhibitor IDN-6556; c-Jun, Jun proto-oncogene; cGAS, cyclic GMP-AMP synthase; DAMP, damage associated molecular pattern; IRF3, interferon regulatory factor 3; ISG, interferon stimulated gene; KSHV, Kaposi's sarcoma-associated herpesvirus; NFKB1, nuclear factor kappa B subunit

32 1 or p50; PAMP, pathogen associated molecular pattern; PRR, pathogen recognition receptor;
33 scRNA-seq, single cell RNA sequencing; STING, stimulator of interferon genes; RelA, RELA
34 proto-oncogene or p65; TBK1, TANK-binding kinase 1; TPA, 12-O-tetradecanoylphorbol-13-
35 acetate or PMA

Abstract

Strict regulation of type I interferons (IFN) is vital for balancing tissue damage and immunity against infections. We previously found that during Kaposi's sarcoma-associated herpesvirus infection, IFN induction was limited to a small percentage of infected B cells. This heterogeneity was not explained by viral gene expression. Here, we used a fluorescent reporter and fluorescence-activated cell sorting to investigate the source of this heterogeneity. Surprisingly, the canonical IFN induction pathway culminating in the activation of the IRF3 transcription factor was similar between cells that made high vs. low/no IFN-β. In contrast, the activation or expression of two other IFN transcription factors, NF-κB and AP-1, correlated with heterogeneous IFN-β induction. Our results suggest that at the level of individual cells, IRF3 is crucial as a pathogen detection signal, but NF-κB and AP-1 are limiting for IFN-β induction.

47 **Introduction**

48 Type I and III interferons such as interferon-β (IFN-β) and interferon-λ (IFN-λ) are
49 potent cytokines that defend mammals against viral infections. As a key component of innate
50 immunity, they orchestrate antiviral defense by signaling through the IFNAR1/2 and
51 IFNLR1/IL10Rβ receptor complexes, respectively, and inducing hundreds of interferon-
52 stimulated genes (ISGs) (1). ISGs encode proteins that modulate cell physiology to antagonize
53 viral replication (2). However, IFNs are well known to be a double-edged sword because of their
54 powerful effects on cell and tissue physiology. While insufficient IFN-related inflammation
55 leaves the host susceptible to infections, excessive IFN-related inflammation causes tissue
56 damage and contributes to autoimmune disease development (3-5). Therefore, IFN-β and other
57 type I and III IFNs are carefully regulated, and multiple host regulatory mechanisms have
58 evolved to ensure their expression only under appropriate conditions.

59 An emerging dimension of IFN regulation is transcriptional heterogeneity at the single-
60 cell level. This aspect of interferon regulation has become clear in the growing number of single-
61 cell RNA sequencing (scRNA-seq) analyses of infected cells. We and others have found only a
62 small percentage (<10%) of virus-infected cells produce IFN-β or IFN-λ (6-18). This has been
63 reported in infections with the RNA viruses Influenza A Virus (7, 10, 11, 14-17), Newcastle
64 Disease Virus (18, 19), West Nile Virus (13), and SARS-CoV-2 (9), as well as the DNA viruses
65 Herpes Simplex Virus 1 (12) and Human Cytomegalovirus (8), in addition to our results with
66 Kaposi's sarcoma-associated herpesvirus (KSHV) (6). Since subversion of type I and III IFN is a
67 key evolutionary tactic for viruses in the virus-host arms race, heterogeneity in the expression
68 and activity of IFN-inhibiting viral proteins has been proposed as the reason for heterogeneous
69 IFN expression (15, 20). However, we and others have found that viral gene expression
70 heterogeneity does not fully account for the observed IFN heterogeneity during infection with
71 KSHV, Influenza A Virus, Sendai Virus, and Newcastle Disease Virus (6, 11, 19, 21, 22),
72 suggesting there are also cellular components to heterogeneous IFN induction. Limiting the
73 percentage of cells producing type I and III IFN in an infected population may allow for optimal
74 distribution of the cytokine and activation of surrounding cells without reaching a dangerous
75 level. However, the mechanisms restricting IFN induction to a few cells remain elusive.

76 Type I and III IFNs are induced in response to pathogen-associated molecular patterns
77 (PAMPs), such as nucleic acids with aberrant characteristics, or damage-associated molecular

78 patterns (DAMPs) due to infection-induced stress. PAMPs and DAMPs are recognized by
79 pattern recognition receptors (PRRs), such as RIG-I-like receptors, Toll-like receptors, and cyclic
80 GMP-AMP synthase (cGAS), which then activate signaling cascades that result in transcription
81 of IFN-β. While different PRRs rely on different signaling adaptors, their signaling pathways
82 generally converge on the kinase TANK-binding kinase 1 (TBK1), which phosphorylates the key
83 transcription factor interferon regulatory factor 3 (IRF3). IRF3 is the best studied IFN-β
84 transcription factor, but IFN-β transcription requires a complex of transcription factor complexes
85 that make up the IFN-β enhanceosome (23). In addition to IRF3, the IFN-β enhanceosome
86 includes the nuclear factor kappa-light-chain-enhancer of activated B-cells (NF-κB) and activator
87 protein 1 (AP-1) complexes. The coordination of multiple transcription factors provides a secure
88 barrier for the appropriate induction of IFN-β. However, how this restriction plays out at the
89 single-cell level remains unknown.

90 Previous studies that have detected IFN-β induction heterogeneity have proposed
91 different explanations. Some studies have suggested that the promoter firing step is inherently
92 stochastic (19, 24). In contrast, Zhao et al. found that the fraction of IFN-β expressing cells
93 remains constant through recloning and cell division, pointing to genetically programmed
94 stochasticity, but were not able to narrow it down to specific factors (21). We previously found
95 that KSHV hijacks the function of host caspases to prevent IFN-β induction when KSHV re-
96 enters the replicative (lytic) cycle from a dormant (latent) infection state (25). Adding a small
97 molecule caspase inhibitor restores activation of the cGAS PRR (6) and results in IFN-β
98 induction (25). While the amount of IFN-β produced under these conditions based on ELISA
99 measurements was substantial (25), subsequent experiments revealed that the IFN-β came from a
100 small population of cells (6). scRNA-seq analysis revealed that IFN-β induction is highly
101 heterogeneous, with less than 4% of infected cells responsible for producing significant amounts
102 of IFN-β (6). The IFN-β heterogeneity was only partially explained by heterogeneous viral gene
103 expression. We did not detect any IFN-β in cells that were latently infected or in the very late
104 stages of lytic replication. We attribute this result to a lack of virus detection in the first case and
105 potent inhibition in the second. However, 46% of the cells had a gene expression pattern
106 corresponding to the early stages of the lytic cycle, but only 6% of them produced IFN-β. When
107 we compared IFN-β positive and negative cells within this group, we did not find any viral gene
108 that was specifically missing in IFN-β-producing cells, as would be expected for a

109 heterogeneously expressed viral IFN suppressor (25). These findings suggested to us that there is
110 an additional, likely cellular, source of IFN-induction heterogeneity in this system.
111 In this study, we used the KSHV lytic infection and caspase inhibition system to probe
112 further the source of heterogeneous IFN-β production during viral infection, as it provides robust
113 and sustained induction of IFN. We developed a tool for separating cells expressing high vs. low
114 levels of IFN-β and found that surprisingly, the canonical IFN induction pathway culminating in
115 IRF3 activation was activated equally in both populations. However, activation or levels of other
116 components of the IFN-β enhanceosome were heterogeneous and better correlated with IFN-β
117 induction. Thus, we establish that in our system, activation of the NF-κB component RelA and
118 baseline levels of the AP-1 component ATF2 are the limiting factors for IFN-β transcription at a
119 single-cell level. This study highlights the nuanced mechanics behind the induction of a key
120 component of our body's antiviral response, and for the first time identifies cellular factors
121 whose heterogeneity contributes to limiting IFN-β induction to a small subpopulation of cells
122 during infection.

123 **Materials and Methods**

124

125 *Cell lines, reagents, and treatments*

126 All cells were cultured at 37°C and 5% CO_2. HEK293T cells were grown in Dulbecco's
127 modified Eagle's medium (DMEM; Life Technologies) supplemented with 10% fetal bovine
128 serum (FBS; Hyclone). BC-3 cells and derivatives were maintained at a density of $0.5x10^6$
129 cells/mL in Roswell Park Memorial Institute medium (RPMI; Life Technologies) supplemented
130 with 20% FBS, 2 mM GlutaMAX (Gibco), and 55 μM β-mercaptoethanol (BME; Gibco). BC-3-
131 IFN-β-tdTomato cells were generated as described in Lent, Tabtieng, et al., 2022 (6). For
132 reactivation, BC-3 cells were seeded at a density of $0.5x10^6$ cells/mL and treated with 20 ng/mL
133 TPA (12-O-tetradecanoylphorbol-13-acetate; MilliporeSigma 5244001MG) dissolved in
134 dimethylsulfoxide (DMSO; Sigma Aldrich Fine Chemicals Biosciences). Reactivation rates were
135 checked for all experiments and are plotted in Supp. Fig. 1). Where indicated, cells were treated
136 with vehicle (DMSO), 10 μM IDN-6556 (Emricasan; Selleck Chemical LLC S777525MG), and
137 a mixture of neutralizing antibodies against type I IFNs at 1:500 dilution (PBS Assay Science
138 39000-1).

139

140 *Fluorescence-activated cell sorting*

141 100 mL of BC-3 cells were seeded at a density of $0.5x10^6$ cells/mL and treated with TPA, IDN-
142 1665, and, where indicated, anti-IFN antibody mixture as described above. After two days, they
143 were collected and sorted based on tdTomato fluorescence on BD FACSAria III at the UW
144 Carbone Cancer Center Flow Cytometry Laboratory core facility. A DAPI stain (which only
145 stains dead cells in the absence of permeabilization) was used to remove dead cells from the
146 analysis. Gates for tdTomato fluorescence were drawn based on a negative control of BC-3 cells
147 that lack the reporter system. BC-3 cells lacking the reporter system were treated identically as
148 the sorted reporter cells. In each experiment, about $80x10^6$ cells were sorted. $3x10^6$ tdTomato+
149 and $12x10^6$ tdTomato- cells were collected. Sorted cells were pelleted and resuspended in 1 mL
150 of PBS each. 100 μL of cell suspension were used for RNA extraction and 900 μL for protein
151 extraction. Bulk controls were prepared in parallel with 4 mL of BC-3 cells seeded at a density of
152 $0.5x10^6$ cells/mL and treated as indicated for 2 days. The bulk control cells were pelleted and

153 resuspended in 1 mL of PBS. 50 µL of cell suspension were used for RNA extraction, 450 µL for
154 protein extraction, and 500 µL for flow cytometry to determine reactivation efficiency.
155
156 *RT-qPCR*
157 RNA samples were collected from BC-3 cells reactivated for 2 days as described above or
158 treated with vehicle. For experiments not involving sorting, 4 mL of BC-3 cells were used and
159 collected as described above for bulk control samples. In both cases, cells to be lysed were
160 pelleted by centrifugation and resuspended in RNA lysis buffer (Zymo research). Total RNA was
161 extracted using the Quick-RNA MiniPrep kit (Zymo research) following the manufacturer's
162 protocol. cDNA was prepared using an iScript cDNA synthesis kit (Bio-Rad) following the
163 manufacturer's protocol. Real-time quantitative PCR (RT-qPCR) was performed using iTaq
164 Universal SYBR green Supermix (Bio-Rad) in a CFX Connect real-time PCR detection system
165 (Bio-Rad). No-template and no-RT controls were included in each replicate. In all cases, 18S
166 rRNA levels were used as an internal standard to calculate relative mRNA levels. CFX Manager
167 software was used to analyze the data. Primers are listed in Table S1.
168
169 *Protein analysis*
170 Protein samples were collected from BC-3 cells reactivated for 2 days as described above or
171 treated with vehicle. For samples not undergoing sorting, 4 mL of BC-3 cells were used and
172 collected as described for bulk control samples. In both cases, cells to be lysed were pelleted by
173 centrifugation and resuspended in an NP-40-only buffer (50 mM Tris-HCl pH 7.4, 150 mM
174 NaCl, 1 mM EDTA, 0.5% NP-40) supplemented with a broad-spectrum protease inhibitor
175 mixture (Thermo Scientific A32955) and a broad-spectrum phosphatase inhibitor mixture
176 (Thermo Scientific A32957). Protein concentration was determined by Bradford method (Bio-
177 Rad 5000006), and Laemmli buffer (Bio-Rad) was added to samples before being denatured at
178 95°C for 5 min. Samples were separated by SDS-PAGE and transferred to polyvinylidene
179 difluoride membranes (PVDF; Fisher Scientific IPFL00010) using semi-dry Trans-Blot Turbo
180 Transfer System (Bio-Rad). Membranes were blocked in 5% bovine serum albumin (BSA;
181 Fisher BioReagents BP1600-100) in TBST. All antibodies used were diluted 1:1000 in 5% BSA
182 in TBST for staining. The following Cell Signaling Technologies antibodies were used: IRF3
183 (D6I4C, no.11904), phospho-IRF3 Ser386 (E7J8G, no.37829), TBK1 (D1B4, no.3504),

184 phospho-TBK1 Ser172 (D52C2, no.5483), ATF2 (D4L2X, no.35031), c-Jun (60A8, no.9165),
185 NF-κB p65/RelA (D14E12, no.8242), phospho-NF-κB p65/RelA Ser536 (93H1, no.3303). In
186 addition, antibodies against β-actin (Abcam, ab8229) were used for loading controls. Secondary
187 horseradish peroxidase (HRP)-conjugated antibodies (goat anti-rabbit and rabbit anti-goat IgG)
188 were purchased from Southern Biotechnology (no.4030-05, no.OB6106-05) and used at 1:5000
189 in 5% BSA in TBST. All membranes were exposed using SuperSignal West Pico PLUS
190 Chemiluminescent Substrate (Thermo Scientific) and imaged with an iBright FL1000 imaging
191 system (Thermo Scientific).
192
193 *Flow cytometry analysis*
194 BC-3-IFN-β-tdTomato cells were fixed with 4% paraformaldehyde (PFA; Electron Microscopy
195 Sciences) in phosphate buffer saline (PBS) for 15 min at room temperature and washed twice
196 with PBS. Then, the cells were permeabilized by incubating in ice cold 90% methanol (diluted in
197 0.5% BSA in PBS) for 5 mins on ice and washed twice with 0.5% BSA in PBS. For
198 measurements of interferon-β reporter activity, cells were then filtered through a 35 μm strainer
199 (Chemglass Life Sciences CLS4380009) and analyzed. For assessment of reactivation efficiency,
200 cells were then stained for a KSHV lytic infection marker, ORF45. They were incubated with
201 antibodies against KSHV ORF45 (Thermo Fisher MA514769) at 1:100 dilution for 1 hr at room
202 temperature, washed twice, and then stained with Alexa Fluor 647 (AF647)-conjugated
203 secondary antibody at 1:500 dilution (Thermo Fisher A21236) for 30 min at room temperature in
204 the dark. 0.5 % BSA in PBS was used for all incubations and washes. After two washes, cells
205 were resuspended in 0.5% BSA in PBS and filtered as above for analysis. Cells were collected
206 by centrifugation at 500 x *g* for 5 min between all washes/incubation. AF647 fluorescence and
207 tdTomato fluorescence were quantified by flow cytometry on a Thermo Fisher Attune NxT V6
208 cytometer at the UWCCC Flow Cytometry Laboratory. AF647 fluorescence was gated based on
209 the corresponding latently infected and vehicle (DMSO)-treated cells. tdTomato fluorescence
210 was gated based on BC-3 cells that lack the reporter system. 300,000 events were collected per
211 sample.
212
213 *Single cell RNA sequencing analysis*

A dataset obtained from KSHV-infected iSLK.219 cells previously published in Lent, Tabtieng, et al., 2022 (6) (GSE190558) was re-analyzed in the current study by extracting prepared Seurat matrices. FindMarkers function of Seurat was used to identify genes whose expression best correlated with IFNB1.

Statistics

All statistical analysis was performed using GraphPad Prism version 10.3.0 or later (GraphPad Software, Boston, MA USA; www.graphpad.com). Statistical significance was determined by One-way ANOVA followed by a *post hoc* multiple-comparison test (Dunnett) when multiple comparisons were required. All data are plotted as means and standard deviations. All plots represent mean +/- standard deviation.

225 **Results**

226

227 *A fluorescent tdTomato reporter driven by a minimal human IFN-β promoter distinguishes cells*
228 *that express high vs. low levels of IFN-β*

229 Using scRNA-seq, we previously found that a very small fraction of KSHV-infected cells
230 produce IFN-β when the virus is reactivated and caspases are inhibited (6). We calculated this
231 fraction to be 3.8% of the total population and 6% of the infected cells in the early stage of the
232 lytic cycle. Nonetheless, the rare IFN-β producing cells clustered together in our scRNA-seq
233 data, suggesting that they have different characteristics from other cell populations. To identify
234 factors involved in IFN-β regulation, we sought to separate and compare IFN-β producing and
235 non-producing cells. We previously engineered a tdTomato reporter driven by two copies of a
236 303 bp minimal promoter sequence from the human *IFNB1* gene (Fig. 1A) and created stable cell
237 lines with this reporter in BC-3 cells, KSHV-infected B cells isolated from a patient with primary
238 effusion lymphoma (BC3-IFN-βp-tdTomato cells) (6). The design of the promoter was based on
239 previous reporters that used two copies of the minimal IFN-β promoter sequence followed by
240 luciferase or chloramphenicol acetyltransferase (26-28). tdTomato was selected because it is the
241 brightest fluorescent protein whose signal is well separated from autofluorescence, which
242 appears in the green channel (29-31). While our original scRNA-seq study was performed in
243 KSHV-infected epithelial cells, the iSLK.219 system (6), we chose BC-3s for subsequent
244 experiments because they are more biologically relevant, as B cells but not epithelial cells are the
245 target of KSHV infection in patients. Moreover, the virus in iSLK.219 cells expresses GFP and
246 RFP fluorescent reporters (32) that restrict our options for fluorescent markers. In BC-3 cells, the
247 KSHV lytic cycle can be reactivated using the protein kinase C activator TPA (Supp. Fig. 1). As
248 we previously reported (6), treating BC3-IFN-βp-tdTomato reporter cells with TPA and the pan-
249 caspase inhibitor IDN-6556 induced IFN-β compared to no treatment, TPA alone, or the caspase
250 inhibitor alone (Fig. 1B). Also as we previously reported (6), we found that only a small
251 percentage of BC3-IFN-βp-tdTomato reporter cells expressed tdTomato (not shown). TPA-
252 mediated reactivation is the most commonly used method of reliably reactivating KSHV in
253 primary effusion lymphoma cell lines such as BC-3 cells (33). However, TPA can drive
254 activation of multiple signaling pathways involved in growth, apoptosis, and differentiation
255 through activation of protein kinase C (34, 35). Therefore, to ensure that the use of TPA would

256 not confound our studies, we measured IFN induction in an uninfected EBV- and KSHV-
257 negative B cell lymphoma line, BJAB cells, treated with TPA and the pan-caspase inhibitor IDN-
258 6556 (36, 37). We found that neither IFN-β nor IFN-λ1 were induced after TPA and IDN-6556
259 treatment in uninfected BJAB cells (Supp. Fig. 3). Therefore, we concluded that the IFN
260 induction in BC-3 cells was indeed due to KSHV lytic reactivation and virus sensing, not just
261 TPA addition, and that this system could be used for further experiments.
262 To isolate cells expressing high and low IFN-β levels, we subjected the lytically
263 reactivated BC3-IFN-βp-tdTomato reporter cells treated with caspase inhibitors to fluorescence-
264 activated cell sorting (FACS) and collected tdTomato+ and tdTomato- cells (Supp. Fig. 2). To
265 confirm that this reporter results in separation of cells based on IFN-β status, we measured
266 tdTomato and IFN-β RNA levels in the sorted samples. Importantly, we found that the
267 endogenous IFN-β transcript was enriched in the tdTomato+ cells and depleted in the tdTomato-
268 cells, as was tdTomato mRNA (Fig. 1C,D). This result demonstrates that FACS of the BC3-IFN-
269 βp-tdTomato reporter line allows us to separate cells producing high and low levels of IFN-β
270 within a population.
271
272 *IFN-β is not stochastically induced*
273 Some groups have proposed that heterogeneous expression of IFN-β may be generated by
274 stochasticity of IFN-β promoter firing (19, 24). This model posits that the signals and activated
275 proteins needed for IFN-β induction are present in all infected cells, but transcription of IFN-β
276 only occurs stochastically in some cells. To test this hypothesis, we took advantage of the fact
277 that pathogen sensing often induces type III IFNs like IFN-λ1 in addition to type I IFNs and that
278 the signaling cascade and transcription factors that regulate type I and III IFNs are very similar
279 (38). However, since IFN-β and IFN-λ1 have separate promoters and are located on different
280 chromosomes, they should not be expressed by the same cells if their transcription upon pathway
281 activation is stochastic. Contrary to the stochasticity model, our results indicated that IFN-β and
282 IFN-λ1 were induced in the same rare cells. We previously reported that based on the scRNA-
283 seq data, IFN-λ1 was also induced in iSLK.219 cells upon lytic reactivation and caspase inhibitor
284 treatment at similar levels to IFN-β (6). We have since performed further analysis of the scRNA-
285 seq data and found that the IFN-λ1 transcript had the closest correlation to the IFN-β transcript.
286 31% of IFN-β-expressing cells also expressed IFN-λ1, compared to only 8% of IFN-β-negative

287 cells (data not shown). We also analyzed IFN-λ1 expression after sorting BC3-IFN-βp-tdTomato
288 cells. Like IFN-β, IFN-λ1 was induced in BC-3 lytic cells treated with caspase inhibitors (Fig.
289 2A). Moreover, IFN-λ1 was enriched and depleted in concert with IFN-β in the tdTomato-
290 positive and negative cells, respectively, indicating that it was likely expressed in the same cells
291 (Fig. 2B). Therefore, we conclude that IFN-β and IFN-λ1 are not stochastically transcribed but
292 coordinately regulated. Moreover, the fact that they are expressed in the same rare subset of
293 KSHV-infected cells suggests that the same upstream determinant leads to heterogeneous type I
294 and III IFN induction.
295
296 *TBK1 and IRF3 activity does not explain IFN-β heterogeneity*
297 The results above suggested that activation of the IFN-β induction pathway rather than
298 IFN-β transcription is heterogeneous. However, there are several signaling steps in this pathway
299 that could be the bottleneck in determining whether cells transcribe IFN-β. Therefore, we
300 monitored the activation of the IFN-β induction pathway, particularly the later steps of kinase
301 and transcription factor activation. We previously found that in our system, IFN-β induction is
302 driven by the DNA sensing cGAS-STING pathway (6) and requires activation of the kinase
303 TBK1 (25). We thus tested whether TBK1 was activated only in the cells that induce IFN-β by
304 comparing levels of phosphorylated TBK1 in lytically reactivated, caspase inhibitor-treated cells
305 sorted based on tdTomato status. We used poly(I:C)-treated A549 cells as positive controls for
306 activation of the pathway. In every experiment, we confirmed that tdTomato-based sorting
307 resulted in the expected enrichment and depletion of IFN-β mRNA in tdTomato+ and tdTomato-
308 cells, respectively (RNA measurements are shown in Fig. 1C). Surprisingly, we observed no
309 difference in activated (phosphorylated) TBK1 between IFN-β high and low cells (Fig. 3). Since
310 TBK1 phosphorylates and activates the well-characterized IFN-β transcription factor IRF3, we
311 also tested whether IRF3 was differentially activated in the IFN-β high vs. low cells. Like TBK1,
312 we observed no difference in IRF3 phosphorylation between the two populations (Fig. 3).
313 Therefore, while both TBK1 and IRF3 were active in lytic cells treated with caspase inhibitors,
314 as expected, their activation alone was not predictive of IFN-β induction (Fig. 3). This result
315 indicates that the canonical IFN induction pathway is activated in many, likely most, infected
316 cells, but that regulation by an important factor besides IRF3 keeps IFN-β induction limited to a
317 small fraction of the population.

318

319 *AP-1 and NF-κB are the determinants of IFN-β heterogeneity*

320 IRF3 activation is often assumed to lead to IFN-β transcription and phosphorylation of IRF3 is
321 commonly used as a proxy for IFN induction. However, the IFN-β enhanceosome contains two
322 additional transcription factor complexes: AP-1, formed by c-Jun and ATF2, and NF-κB, formed
323 by the RelA/p65 and NFKB1/p50 subunits (39-41). While the AP-1 and NF-κB complexes in
324 other settings can include other members of the c-Jun, ATF2, and NF-κB families, the specific
325 proteins listed above are required for IFN-β transcription during viral infections (41). Moreover,
326 at least NF-κB and IRF3 are also transcription factors for IFN-λ1 (42). However, the exact
327 pathways activating AP-1 and NF-κB in the IFN-β induction pathway and their relation to
328 activation of cGAS and other PRRs are not well understood. Given that IRF3 activation did not
329 explain IFN-β heterogeneity, we considered the possibility that AP-1 and/or NF-κB might be the
330 determinants of heterogeneous IFN-β induction in our system. We previously reported that the
331 expression of NF-κB family members was enriched in IFN-β-expressing cells based on scRNA-
332 seq analysis of KSHV-infected iSLK.219 cells treated with caspase inhibitors (6). We reanalyzed
333 the scRNA-seq dataset and found that this was also the case for the AP-1 components (not
334 shown). To further explore the relationship between IFN-β and these transcription factors, we
335 focused on the IFN-β producing cells by separating the IFN-β expressing clusters (clusters 9 and
336 11) into IFN-β-positive and negative cells (Fig. 4A). Both the NF-κB components RelA and
337 NFKB1/p50 and the AP-1 component c-Jun were enriched in the IFN-β-positive cells (Fig. 4A).
338 This enrichment was particularly evident when anti-interferon blocking antibodies were added to
339 prevent paracrine and autocrine signaling from IFN-β, because most of these genes were induced
340 by IFN-β signaling (Fig. 4B). To note, we also observed an enrichment of IRF3 RNA in the IFN-
341 β-producing cells in the scRNA-seq data, even though we did not detect enrichment at the
342 protein level in BC-3 cells (Fig. 3B). We then tested whether NF-κB and AP-1 were enriched at
343 the protein level in BC-3 cells expressing high levels of IFN-β. To reduce confounds from
344 paracrine signaling, we repeated the sorting experiments with anti-IFN blocking antibodies. The
345 antibody treatment effectively blocked responses to IFN, as shown by a reduction in the levels of
346 the IFN-stimulated gene MxA (Supp. Fig. 1C). We still observed IFN-β induction in the lytic
347 cells treated with caspase inhibitors after antibody treatment, although it was decreased (Fig.
348 4C), which was consistent with our results in iSLK.219 cells (6). It is likely that the anti-IFN

349 blocking antibodies prevent a positive feedback mechanism that enhances IFN-β induction (43).
350 Importantly, we still observed enrichment of IFN-β RNA in the sorted tdTomato+ reporter cells,
351 and similar levels of total and phosphorylated IRF3 in both tdTomato+ and tdTomato- cells (Fig.
352 4D,E). In contrast, we observed an enrichment in the AP-1 component ATF2 in tdTomato+ vs.
353 tdTomato- cells, indicating that ATF2 levels are higher in cells that express high levels of IFN-β
354 (Fig. 4F). Interestingly, total ATF2 levels did not change between conditions in unsorted (bulk)
355 samples, indicating that ATF2 expression was not induced during infection and/or by caspase
356 inhibitor treatment. Instead, these results suggest that basal expression of ATF2 is variable and
357 that IFN-producing cells had higher ATF2 levels prior to lytic reactivation (Fig. 4F). Levels of
358 the other AP-1 component c-Jun were variable across replicates, but in two out of three replicates
359 a unique shorter isoform was detected in the sorted IFN-β high cells (Fig. 4F). However, this
360 shorter c-Jun isoform was also induced by treatment of uninfected BJAB cells treated with TPA
361 and caspase inhibitors (Supp. Fig. 3C), suggesting that its appearance may be unrelated to viral
362 replication and IFN induction, as IFN-β is not induced in uninfected cells (Supp. Fig. 3A). In
363 addition, sorting for IFN-β high cells enriched for cells containing phosphorylated RelA, one of
364 the NF-κB components, whereas there was little to no phosphorylated RelA in the IFN-β low
365 cells. This result points to RelA activation only in IFN-β high cells (Fig. 4G). Overall, these
366 results point to a role for ATF2 and phospho-RelA in cell-specific IFN-β induction. Moreover,
367 our results indicate that elevated ATF2 levels are likely a predictor of IFN-β induction, while
368 RelA is likely activated in response to a stimulus but may serve to potentiate IFN transcription
369 (Fig. 5).

370 **Discussion**

371 In this study, we reveal that the IFN-β enhanceosome components AP-1 and NF-κB, but
372 not IRF3, determine whether individual cells induce IFN-β during KSHV and caspase inhibition.
373 We found that protein levels of the AP-1 factor ATF2 and phosphorylation of the NF-κB factor
374 RelA are higher in cells that express high levels of IFN-β than in cells that express minimal IFN-
375 β. In particular, ATF2 levels are not upregulated under IFN-inducing conditions based on bulk
376 analysis, but our results indicate that sorting for cells with high IFN-β enriched for cells with
377 high ATF2. The implication of this finding is that ATF2 heterogeneity precedes viral reactivation
378 and only cells with higher ATF2 are able to respond to pathogen cues by turning on IFN-β. In
379 contrast, RelA is only activated under IFN-inducing conditions, which suggests a possible
380 bottleneck to its activation in most cells. Our findings thus support a model in which IFN-β
381 inducibility during KSHV lytic replication is limited to a rare fraction of cells with baseline
382 elevated ATF2 levels, and the ability to activate NF-κB. While IRF3, AP-1, and NF-κB have
383 long been known to regulate IFN transcription, their heterogeneity at the single-cell level had not
384 previously been reported. Moreover, this is the first description of the unique role of AP-1 and
385 NF-κB in controlling which individual cells make IFN.

386 Host regulation of IFN-β is important given its potent effects on both the host and
387 pathogen through autocrine and paracrine induction of hundreds of ISGs. Insufficient induction
388 of ISGs can lead to susceptibility to infection, while excessive IFN-related inflammation can lead
389 to autoimmune disorders and excessive tissue damage. A system in which the barrier for IFN-β
390 induction is very high may provide an appropriate level of innate immune alarm by limiting IFN-
391 β expression to a small fraction of infected cells. The fact that many viral infections display
392 heterogeneous IFN induction in a way that is not fully explained by viral factors (11, 19, 21, 22),
393 in combination with our results, suggests that an important part of the mechanism of IFN
394 regulation is rooted in cellular heterogeneity. Furthermore, heterogeneous expression of other
395 cytokines such as IL-2 (44), IL-4 (45, 46), IL-5 (47), and IL-10 (48) has been reported,
396 suggesting this is an important mode of immune regulation.

397 Interestingly, while IRF3 and TBK1 are required for IFN induction following
398 PAMP/DAMP signaling, here we found they are not sufficient. Although IRF3 activation is
399 often used as a proxy for IFN-β induction, especially in studies of viral infections, our results
400 indicate that this one-to-one relationship is not true at the level of individual cells. Indeed, both

401 TBK1 and IRF3 appear to be activated regardless of the IFN status of the cells. Most likely, the
402 upstream components of the IFN induction pathway, including the PRR (cGAS in this case), are
403 also activated regardless of the IFN status of the cells. Instead, our results point to the other IFN-
404 β enhanceosome factors, AP-1 and NF-κB, as the limiting factors that determine IFN-β induction
405 in individual cells. We propose a model where IRF3 serves as an indicator for infection, while
406 AP-1 and NF-κB heterogeneity function to limit IFN-β induction to a small subset of cells
407 among an infected population.

408 The regulation of AP-1 and NF-κB during IFN responses is not as well characterized as
409 the activation of IRF3, although NF-κB is likely also activated downstream of STING (49). For
410 AP-1, our results suggest that differences may precede infection, because at the bulk level there
411 is no clear change in ATF2 levels. Therefore, the simplest interpretation for our results (Fig. 5) is
412 that some cells have higher ATF2, and these cells are more abundant in the IFN-producing pool.
413 In contrast, NF-κB is likely activated in a subset of cells under IFN-inducing conditions. While
414 IRF3 and NF-κB may both be activated by STING (49), the fact that NF-κB is only
415 phosphorylated in IFN-β high cells while IRF3 is phosphorylated equally in IFN-β high and low
416 cells indicates that there must be a heterogenous bottleneck downstream of STING specifically
417 for NF-κB activation.

418 While this study has shed light on the expression mechanics of IFN-β during KSHV
419 infection, the mechanism of IFN heterogeneity may differ in other viral infections and cell types.
420 Although IFN heterogeneity is a widespread feature of viral infection, reported by every study
421 we have encountered, the PRRs and signaling pathways that lead to IFN induction vary (6-18,
422 50). Moreover, IFN-β expression patterns appear to differ between cell types. For example, a
423 larger proportion of infected dendritic cells expresses IFN-β (19, 51, 52) compared to other cell
424 types, such as fibroblasts and epithelial cells (6-16). Flexibility in tailoring the IFN response to
425 factors such as cell type, viral load, and PAMP type is likely evolutionarily beneficial in
426 mounting an appropriate immune response. More studies identifying the determinants of IFN
427 expression are needed to parse out the ubiquity vs. uniqueness of our findings.

428 Although our findings indicate that there is a high barrier to IFN-β induction, results from
429 studies using Sendai virus suggest that heterogeneity of IFN-β induction is not due to a complete
430 inability of some cells to induce IFN-β. Infection with a highly inflammatory strain of Sendai
431 virus (the Cantell strain) induced IFN-β expression in 99% of infected A549 cells (11, 52). In

432 comparison, only 0.48% of A549 cells expressed IFN-β during infection with influenza A virus
433 (11). This indicates that IFN-β regulation can be overridden given excessive stimuli such as the
434 defective-interfering viral genomes that characterize the Sendai virus strain Cantell (53). These
435 observations also suggest that the strength or abundance of the stimulus may matter. Indeed,
436 strong IFN inducers like Newcastle Disease Virus, Sendai virus strain Cantell, or the potent
437 PAMP mimetic poly(I:C) induce IFN-β in a larger proportion of cells (10-99%) (21, 22, 50, 51,
438 54-57) compared to other viral infections and treatments (1-10%) (6-17). Unfortunately, we have
439 been unable to test whether the relationship between the strength of the stimulus and the
440 percentage of IFN-expressing cells is also true in KSHV-infected BC-3 cells, as we have not
441 identified a stronger stimulus that worked in this line. In order to isolate the cells that express
442 IFN-β, the cells need to be active and viable for long enough for the tdTomato fluorescent
443 protein to express and accumulate to detectable levels. Commonly used IFN-inducing stimuli
444 (poly(I:C), 2'3'-cGAMP, STING agonist diABZI, TLR7 agonist imiquimod, and plasmid DNA)
445 either did not induce IFN-β expression in BC-3 cells or induced cell death before we could assess
446 tdTomato production (data not shown). IFN-β induction through KSHV reactivation and caspase
447 inhibition allows for sustained IFN-β induction without inducing cell death, which gives us a
448 unique tool to study the elusive phenomena of cellular heterogeneity and IFN-β induction.
449 There are some limitations to our study. First, the minimal IFN-β promoter used in our
450 reporter lacks the native chromatin environment and potential long-range promoter elements.
451 Our reporter system also did not fully recapitulate IFN-β kinetics, as only cells that had sustained
452 IFN-β promoter activity were detectable during FACS. However, despite these imperfections, we
453 were able to successfully separate the rare cells that expressed high levels of IFN-β (Fig. 1C).
454 Also, while our results point to cellular heterogeneity as a major determinant of IFN-β
455 regulation, we cannot completely rule out the possibility that the heterogeneity of AP-1 and NF-
456 κB is regulated by the virus. While our scRNA-seq data did not reveal any correlation between
457 viral genes and IFN-β expression (6), this method does not capture mutations that may have risen
458 in individual cells. Moreover, the sequencing method was 3' end-directed, and many mRNAs in
459 KSHV share 3' end sequences, preventing accurate measurement of some viral genes. We have
460 also not repeated the scRNA-seq in the BC-3 cells. That said, to date there has been no report of
461 a KSHV factor that blocks NF-κB activation in response to PRR activation or that regulates AP-
462 1 levels, so there is no obvious viral explanation for the heterogeneity we observe. Lastly, while

463 TPA is a very effective inducer of lytic KSHV reactivation and is commonly used in KSHV
464 research (33), it is also a known inducer of NF-κB in other setting. This is a potentially
465 confounding variable. Our concern about this is reduced by the fact that treatments that induced
466 IFN-β in infected BC-3 cells did not induce IFN-β or RelA phosphorylation in the uninfected
467 BJAB cells, indicating that viral infection and not TPA treatment induces IFN-β. Moreover, our
468 results are consistent between the BC-3 and iSLK.219 KSHV-infected cell lines, even though
469 iSLK.219 cells are not treated with TPA to induce the lytic cycle. This also suggests that our
470 results are not simply due to TPA treatment.

471 Despite the described limitations, this study points us to a new model of heterogeneous
472 type I IFN transcription during viral infection as the result of inherent cellular heterogeneity in
473 protein levels and protein activation. It is the first report of a role for cellular transcription factors
474 in IFN induction heterogeneity. More studies are needed to pinpoint the earliest source of the
475 heterogeneity and to examine the mechanism of enrichment and activation of AP-1 and NF-κB in
476 the context of antiviral responses.
477

478 **Acknowledgements**
479 We thank members of the Gaglia laboratory for suggestions and feedback on the project and the
480 manuscript. We thank the University of Wisconsin Carbone Cancer Center (UWCCC) Flow
481 Cytometry Laboratory staff for technical and conceptual assistance.

482 **References**

483 1. Schoggins, J. W., S. J. Wilson, M. Panis, M. Y. Murphy, C. T. Jones, P. Bieniasz, and C.
484 M. Rice. 2011. A diverse array of gene products are effectors of the type I interferon
485 antiviral response. *Nature* 472.
486 2. Schoggins, J. W., and C. M. Rice. 2011. Interferon-stimulated genes and their antiviral
487 effector functions. *Curr Opin Virol* 1: 7.
488 3. Taft, J., and D. Bogunovic. 2018. The Goldilocks Zone of Type I IFNs: Lessons from
489 Human Genetics. *J Immunol* 201: 7.
490 4. González-Navajas, J. M., J. Lee, M. David, and E. Raz. 2012. Immunomodulatory
491 functions of type I interferons. *Nat Rev Immunol* 12: 11.
492 5. Kobayashi, K. S., and R. A. Flavell. 2004. Shielding the double-edged sword: negative
493 regulation of the innate immune system. *J Leukoc Biol* 75: 6.
494 6. Tabtieng, T., R. C. Lent, M. Kaku, A. Monago Sanchez, and M. M. Gaglia. 2022.
495 Caspase-Mediated Regulation and Cellular Heterogeneity of the cGAS/STING Pathway
496 in Kaposi's Sarcoma-Associated Herpesvirus Infection. *mBio* e0244622.
497 7. Hamele, C. E., A. B. Russell, and N. S. Heaton. 2022. In Vivo Profiling of Individual
498 Multiciliated Cells during Acute Influenza A Virus Infection. *J Virol* 96.
499 8. Hein, M. Y., and J. S. Weissman. 2022. Functional single-cell genomics of human
500 cytomegalovirus infection. *Nat Biotechnol* 40: 11.
501 9. Fiege, J. K., J. M. Thiede, H. A. Nanda, W. E. Matchett, P. J. Moore, N. R. Montanari, B.
502 K. Thielen, J. Daniel, E. Stanley, R. C. Hunter, V. D. Menachery, S. S. Shen, T. D. Bold,
503 and R. A. Langlois. 2021. Single cell resolution of SARS-CoV-2 tropism, antiviral
504 responses, and susceptibility to therapies in primary human airway epithelium. *PLoS*
505 *Pathog* 17.
506 10. Sun, J., J. C. Vera, J. Drnevich, Y. T. Lin, R. Ke, and C. B. Brooke. 2020. Single cell
507 heterogeneity in influenza A virus gene expression shapes the innate antiviral response to
508 infection. *PLoS Pathog* 16.
509 11. Russell, A. B., E. Elshina, J. R. Kowalsky, A. J. W. Te Velthius, and J. D. Bloom. 2019.
510 Single-Cell Virus Sequencing of Influenza Infections That Trigger Innate Immunity. *J*
511 *Virol* 93.

512 12. Drayman, N., P. Patel, L. Vistain, and S. Tay. 2019. HSV-1 single-cell analysis reveals
513 the activation of anti-viral and developmental programs in distinct sub-populations. *Elife*
514 8.
515 13. O'Neal, J. T., A. Upadhyay, A. Wolabaugh, N. B. Patel, S. E. Bosinger, and M. S.
516 Suthar. 2019. West Nile Virus-Inclusive Single-Cell RNA Sequencing Reveals
517 Heterogeneity in the Type I Interferon Response within Single Cells. *J Virol* 93.
518 14. Russell, A. B., C. Trapnell, and J. D. Bloom. 2018. Extreme heterogeneity of influenza
519 virus infection in single cells. *Elife* 7.
520 15. Killip, M. J., R. Jackson, M. Pérez-Cidoncha, E. Fodor, and R. E. Randall. 2017. Single-
521 cell studies of IFN-β promoter activation by wild-type and NS1-defective influenza A
522 viruses. *J Gen Virol* 98: 7.
523 16. Pérez-Cidoncha, M., M. J. Killip, J. C. Oliveros, V. J. Asensio, Y. Fernández, J. A.
524 Bengoechea, R. E. Randall, and J. Ortín. 2014. An unbiased genetic screen reveals the
525 polygenic nature of the influenza virus anti-interferon response. *J Virol* 88: 15.
526 17. Kallfass, C., S. Lienenklaus, S. Weiss, and P. Staeheli. 2013. Visualizing the beta
527 interferon response in mice during infection with influenza A viruses expressing or
528 lacking nonstructural protein 1. *J Virol* 87: 6.
529 18. Hu, J., G. Nudelman, Y. Shimoni, M. Kumar, Y. Ding, C. López, F. Hayot, J. G.
530 Wetmur, and S. Sealfon. 2011. Role of cell-to-cell variability in activating a positive
531 feedback antiviral response in human dendritic cells. *PLoS One* 6.
532 19. Hu, J., S. Sealfon, F. Hayot, C. Jayaprakash, M. Kumar, A. C. Pendleton, A. Ganee, A.
533 Fernandez-Sesma, T. M. Moran, and J. G. Wetmur. 2007. Chromosome-specific and
534 noisy IFNB1 transcription in individual virus-infected human primary dendritic cells.
535 *Nucleic Acids Res* 35: 10.
536 20. Chen, S., J. A. L. Short, D. F. Young, M. J. Killip, M. Schneider, S. Goodbourn, and R.
537 E. Randall. 2010. Heterocellular induction of interferon by negative-sense RNA viruses.
538 *Virology* 407.
539 21. Zhao, M., J. Zhang, H. Phatnani, S. Scheu, and T. Maniatis. 2012. Stochastic expression
540 of the interferon-β gene. *PLoS Biol* 10.

541 22. Rand, U., M. Rinas, J. Schwerk, G. Nöhren, M. Linnes, A. Kröger, M. Flossdorf, K.
542 Kály-Kullai, H. Hauser, T. Höfer, and M. Köster. 2012. Multi-layered stochasticity and
543 paracrine signal propagation shape the type-I interferon response. *Mol Syst Biol* 8.
544 23. Panne, D., T. Maniatis, and S. C. Harrison. 2007. An atomic model of the interferon-beta
545 enhanceosome. *Cell* 129: 13.
546 24. Apostolou, E., and D. Thanos. 2008. Virus Infection Induces NF-kappaB-dependent
547 interchromosomal associations mediating monoallelic IFN-beta gene expression. *Cell*
548 134: 7.
549 25. Tabtieng, T., A. Degterev, and M. M. Gaglia. 2018. Caspase-Dependent Suppression of
550 Type I Interferon Signaling Promotes Kaposi's Sarcoma-Associated Herpesvirus Lytic
551 Replication. *J Virol* 92.
552 26. Li, K., Z. Chen, N. Kato, K. Gale, and S. M. Lemon. 2005. Distinct poly(I-C) and virus-
553 activated signaling pathways leading to interferon-beta production in hepatocytes. *J Biol*
554 *Chem* 280: 9.
555 27. Guo, F., J. Mead, N. Aliya, L. Wang, A. Cuconati, L. Wei, K. Li, T. M. Block, J. T. Guo,
556 and J. Chang. 2012. RO 90-7501 enhances TLR3 and RLR agonist induced antiviral
557 response. *PLoS One* 7.
558 28. Gentili, M., J. Kowal, M. Tkach, T. Satoh, X. Lahaye, C. Conrad, M. Boyron, B.
559 Lombard, S. Durand, G. Kroemer, D. Loew, M. Dalod, C. Thery, and N. Manel. 2015.
560 Transmission of innate immune signaling by packaging of cGAMP in viral particles.
561 *Science* 349.
562 29. Day, R. N., and M. W. Davidson. 2009. The fluorescent protein palette: tools for cellular
563 imaging. *Chem Soc Rev* 38: 34.
564 30. Muzumdar, M. D., B. Tasic, K. Miyamichi, L. Li, and L. Luo. 2007. A global double-
565 fluorescent Cre reporter mouse. *Genesis* 45: 13.
566 31. Surre, J., C. Saint-Ruf, V. Collin, S. Orenga, M. Ramjeet, and I. Matic. 2018. Strong
567 increase in the autofluorescence of cells signals struggle for survival. *Sci Rep* 8.
568 32. Brulois, K. F., H. Chang, A. S. Y. Lee, A. Ensser, L. Y. Wong, Z. Toth, S. H. Lee, H. R.
569 Lee, J. Myoung, D. Ganem, T. K. Oh, J. F. Kim, S. J. Gao, and J. U. Jung. 2012.
570 Construction and Manipulation of a New Kaposi's Sarcoma-Associated Herpesvirus
571 Bacterial Artificial Chromosome Clone. *J Virol* 86.

572 33. Cohen, A., C. Brodie, and R. Sarid. 2006. An essential role of ERK signalling in TPA-
573 induced reactivation of Kaposi's sarcoma-associated herpesvirus. *J Gen Virol* 87: 8.
574 34. Kikkawa, U., H. Matsuzaki, and T. Yamamoto. 2002. Protein kinase C delta (PKC delta):
575 activation mechanisms and functions. *J Biochem* 132: 9.
576 35. Duquesnes, N., F. Lezoualc'h, and B. Crozatier. 2011. PKC-delta and PKC-epsilon: foes
577 of the same family or strangers? *J Mol Cell Cardiol* 51: 9.
578 36. Menezes, J., W. Leibold, G. Klein, and G. Clemens. 1975. Establishment and
579 characterization of an Epstein-Barr virus (EBC)-negative lymphoblastoid B cell line
580 (BJA-B) from an exceptional, EBV-genome-negative African Burkitt's lymphoma.
581 *Biomedicine* 22: 9.
582 37. Arvanitakis, L., E. A. Mesri, R. G. Nador, J. W. Said, A. S. Asch, D. M. Knowles, and E.
583 Cesarman. 1996. Establishment and characterization of a primary effusion (body cavity-
584 based) lymphoma cell line (BC-3) harboring kaposi's sarcoma-associated herpesvirus
585 (KSHV/HHV-8) in the absence of Epstein-Barr virus. *Blood* 88.
586 38. Onoguchi, K., M. Yoneyama, A. Takemura, S. Akira, T. Taniguchi, H. Namiki, and T.
587 Fujita. 2007. Viral infections activate types I and III interferon genes through a common
588 mechanism. *J Biol Chem* 282: 6.
589 39. Lenardo, M. J., C. M. Fan, T. Maniatis, and D. Baltimore. 1989. The involvement of NF-
590 kappa B in beta-interferon gene regulation reveals its role as widely inducible mediator of
591 signal transduction. *Cell* 57: 8.
592 40. Wathelet, M. G., C. H. Lin, B. S. Parekh, L. V. Ronco, P. M. Howley, and T. Maniatis.
593 1998. Virus infection induces the assembly of coordinately activated transcription factors
594 on the IFN-beta enhancer in vivo. *Mol Cell* 1: 11.
595 41. Maniatis, T., J. V. Falvo, T. H. Kim, T. K. Kim, C. H. Lin, B. S. Parekh, and M. G.
596 Wathelet. 1998. Structure and function of the interferon-beta enhanceosome. *Cold Spring*
597 *Harb Symp Quant Biol* 63: 12.
598 42. Iversen, M. B., and S. R. Paludan. 2010. Mechanisms of type III interferon expression. *J*
599 *Interferon Cytokine Res* 30: 6.
600 43. Ma, F., B. Li, S. Liu, S. S. Iyer, Y. Yu, A. Wu, and G. Cheng. 2015. Positive feedback
601 regulation of type I IFN production by the IFN-inducible DNA sensor cGAS. *194* 4: 10.

602 44. Holländer, G. A. 1999. On the stochastic regulation of interleukin-2 transcription. *Semin*
603 *Immunol* 11: 11.
604 45. Guo, L., J. Hu-Li, and W. E. Paul. 2004. Probabilistic regulation of IL-4 production in
605 Th2 cells: accessibility at the Il4 locus. *Immunity* 20: 11.
606 46. Guo, L., J. Hu-Li, and W. E. Paul. 2005. Probabilistic regulation of IL-4 production. *J*
607 *Clin Immunol* 25: 9.
608 47. Kelly, B. L., and R. M. Locksley. 2000. Coordinate regulation of the IL-4, IL-13, and IL-
609 5 cytokine cluster in Th2 clones revealed by allelic expression patterns. *J Immunol* 165:
610 5.
611 48. Calado, D. P., T. Paixão, D. Holmberg, and M. Haury. 2006. Stochastic monoallelic
612 expression of IL-10 in T cells. *J Immunol* 177: 7.
613 49. Ishikawa, H., and G. N. Barber. 2008. STING is an endoplasmic reticulum adaptor that
614 facilitates innate immune signalling. *Nature* 455: 5.
615 50. Parekh, N., D. Winship, E. V. Dis, and D. B. Stetson. 2024. Regulation and Dynamics of
616 IFN-β Expression Revealed with a Knockin Reporter Mouse. *J Immunol* 213: 11.
617 51. Shalek, A. K., R. Satija, J. Shuga, J. J. Trombetta, D. Gennert, D. Lu, P. Chen, R. S.
618 Gertner, J. T. Gaublomme, N. Yosef, S. Schwartz, B. Fowler, S. Weaver, J. Wang, X.
619 Wang, R. Ding, R. Raychowdhury, N. Friedman, N. Hacohen, H. Park, A. P. May, and A.
620 Regev. 2014. Single-cell RNA-seq reveals dynamic paracrine control of cellular
621 variation. *Nature* 510: 7.
622 52. Strahle, L., D. Garcin, and D. Kolakofsky. 2006. Sendai virus defective-interfering
623 genomes and the activation of interferon-beta. *Virology* 351: 11.
624 53. Johnston, M. D. 1981. The characteristics required for a Sendai virus preparation to
625 induce high levels of interferon in human lymphoblastoid cells. *J Gen Virol* 56: 10.
626 54. Patil, S., M. Fribourg, Y. Ge, M. Batish, S. Tyagi, F. Hayot, and S. Sealfon. 2015. Single-
627 cell analysis shows that paracrine signaling by first responder cells shapes the interferon-
628 β response to viral infection. *Sci Signal* 8.
629 55. Hwang, S. Y., K. Y. Hur, J. R. Kim, K. H. Cho, S. H. Kim, and J. Y. Yoo. 2013. Biphasic
630 RLR-IFN-β response controls the balance between antiviral immunity and cell damage. *J*
631 *Immunol* 190: 9.

632 56. Zawatzky, R., E. D. Maeyer, and J. D. Maeyer-Guignard. 1985. Identification of
633 individual interferon-producing cells by in situ hybridization. *PNAS* 82: 5.
634 57. Enoch, T., K. Zinn, and T. Maniatis. 1986. Activation of the human beta-interferon gene
635 requires an interferon-inducible factor. *Mol Cell Biol* 6: 10.
636

637 **Figure legends**

638

639 **Figure 1. An IFN-β-promoter driven fluorescent reporter allows isolation of cells**
640 **expressing high and low levels of IFN-β. A.** Diagram of the IFN-βp-tdTomato reporter. Two
641 copies of the 303 bp minimal promoter sequence for the human IFNB1 gene were cloned in front
642 of the tdTomato fluorophore. This cassette was then introduced in BC-3 cells via lentiviral
643 transduction leading to stable integration. **B-D.** BC3-IFN-βp-tdTomato reporter cells were
644 treated with 20 ng/mL TPA for 48 hours to induce the lytic cycle ("lytic (TPA)") Where
645 indicated, the cells were also treated with the pan-caspase inhibitor IDN-6556 at 10 μM ("casp-
646 i"). IFN-β and tdTomato mRNA levels were measured by RT-qPCR and normalized to 18S
647 rRNA. For **B**, IFN-β mRNA levels are plotted normalized to the lytic+casp-i sample. For **C and**
648 **D** the lytic+casp-i treated samples were sorted based on tdTomato expression and the fold
649 enrichment in IFN-β and tdTomato RNA levels compared to unsorted ("bulk") samples is plotted
650 in $\log_{10}$ scale. n=6.

651

652 **Figure 2. IFN-λ1 is expressed in the same set of cells that produce high levels of IFN-β,**
653 **pointing to heterogeneity in the induction pathway rather than -stochastic IFN-β promoter**
654 **firing. A.** BC3-IFN-βp-tdTomato reporter cells were treated with 20 ng/ml TPA for 48 hours to
655 induce the lytic cycle ("lytic (TPA)"). Where indicated, the cells were also treated with the pan-
656 caspase inhibitor IDN-6556 at 10 μM ("casp-i"). IFN-λ1 mRNA was measured by RT-qPCR and
657 normalized to 18S rRNA. For **A,** IFN-λ1 mRNA levels are plotted normalized to the lytic+casp-i
658 sample. In **B,** the lytic+casp-i treated samples were sorted based on tdTomato expression and the
659 fold enrichment in IFN-λ1 RNA levels compared to unsorted ("bulk") samples is plotted in $\log_{10}$
660 scale. n=6.

661

662 **Figure 3. TBK1 and IRF3 are activated even in cells that do not transcribe IFN-β.** BC3-
663 IFN-βp-tdTomato reporter cells were treated with 20 ng/ml TPA for 48 hours to induce the lytic
664 cycle ("lytic (TPA)"). Where indicated, the cells were also treated with the pan-caspase inhibitor
665 IDN-6556 at 10 μM ("casp-i"). Protein was isolated from treated cells without sorting ("bulk"),
666 or, for the lytic+casp-i treated sample, after sorting based on tdTomato expression. Protein
667 lysates were probed for phosphorylated IRF3 (Ser386), total IRF3, phosphorylated TBK1

668 (Ser172), total TBK1, and β-actin as a loading control. As a positive control for IRF3 and TBK1
669 activation/phosphorylation, A549 cells were treated with poly(I:C) for 6 and 48 hours before
670 protein lysates were collected. Images shown are representative of 3 replicates.
671
672 **Figure 4. Levels of the AP-1 subunit ATF2 and phosphorylation of the NF-κB subunit RelA**
673 **are higher in IFN-β high cells. A-B.** Re-analysis of single-cell RNA sequencing (scRNA-seq)
674 data in Tabtieng, Lent et al 2022 (6). iSLK.219 cells were treated with 1 μg/mL doxycycline for
675 4 days to induce the lytic cycle ("lytic"). The cells were also treated with the pan-caspase
676 inhibitor IDN-6556 at 10 μM ("casp-i"), as well as a mixture of antibodies against type I
677 interferon and its receptor ("anti-IFN Abs") (**B** only) to block IFN-β paracrine signaling where
678 indicated. Average mRNA levels of genes in the IFN-β enhanceosome from the scRNA-seq data
679 are shown for each of the 12 clusters of cells identified by the original analysis. The IFN-β-
680 positive clusters 9 and 11 were further separated into two groups based on the IFN-β status of
681 individual cells. **C-G.** BC3-IFN-βp-tdTomato reporter cells were treated with 20 ng/ml TPA for
682 48 hours to induce the lytic cycle ("lytic (TPA)"). Where indicated, the cells were also treated
683 with the pan-caspase inhibitor IDN-6556 at 10 μM ("casp-i") and with a mixture of antibodies
684 against type I interferon and its receptor ("anti-IFN Abs") to block IFN-β paracrine signaling.
685 The lytic+casp-i+anti-IFN Abs treated samples were also sorted based on tdTomato expression
686 in D-G. **C-D.** IFN-β RNA was measured by RT-qPCR and normalized to 18S rRNA. In C, IFN-β
687 RNA levels are plotted normalized to the lytic+casp-i sample. In D, the fold enrichment in IFN-β
688 RNA levels is compared to unsorted ("bulk") samples plotted in $\log_{10}$ scale. n=4. **E-G.** Western
689 blots of protein samples from unsorted ("bulk") and sorted cells. Protein lysates were probed for:
690 (**E**) phosphorylated IRF3 (Ser386), total IRF3, (**F**) ATF2, c-Jun, (**G**) phosphorylated RelA
691 (Ser536), total RelA, β-actin was used as loading control. Images shown are representative of 3
692 replicates.
693
694 **Figure 5. Model of regulation of heterogeneous IFN-β expression by components of the**
695 **IFN-β enhanceosome.** *(Left)* In the rare cells that induce IFN-β during viral infection, there are
696 high levels of the AP-1 factor ATF2 and the NF-κB subunit RelA becomes phosphorylated in
697 addition to IRF3 in response to infection. This results in the formation of the IFN-β
698 enhanceosome and IFN-β transcription. *(Right)* In the majority of virally infected cells, there are

699 lower amounts of ATF2, and RelA is not phosphorylated during infection. While IRF3 is still
700 activated, the full IFN-β enhanceosome does not form and IFN-β is not induced.
701
702 **Supplemental Figure 1. Controls showing efficient reactivation of BC3-IFN-βp-tdTomato**
703 **and efficient block of interferon stimulate gene induction by anti-IFN antibodies.** BC3-IFN-
704 βp-tdTomato reporter cells were treated with 20 ng/ml TPA for 48 hours to induce the lytic cycle
705 ("lytic"). Where indicated, the cells were also treated with the pan-caspase inhibitor IDN-6556 at
706 10 μM ("casp-i") and in **B and C** a mixture of antibodies against type I interferon and its
707 receptor ("anti-IFN Abs") to block IFN-β paracrine signaling. The percentage of cells expressing
708 the lytic KSHV protein ORF45 was measured by flow cytometry. Graphs A and B show the
709 reactivation rates for all BC3 experiments shown (**A)** n=7, (**B**) n=5. **C.** mRNA levels of MxA, an
710 interferon stimulated gene (ISG) were measured by qRT-PCR and normalized to 18S rRNA.
711 n=4.
712
713 **Supplemental Figure 2. Representative gating strategy for FACS.** Plots showing an example
714 gating for BC3-IFN-βp-tdTomato cell sorting based on tdTomato fluorescence. Gates for
715 tdTomato-positive and negative populations were drawn conservatively to prevent false positives
716 and negatives. In this particular experiment, BC3-IFN-βp-tdTomato reporter cells were treated
717 with 20 ng/ml TPA and 10 μM IDN-6556 (IDN) for 48 hours to induce the lytic cycle and trigger
718 IFN-β expression and tdTomato production. Side scatter (SSC) and forward scatter (FSC) area
719 (A) and height (H) were used to separate cells from debris and remove doublets. DAPI staining
720 was used to identify live cells. Cells thus gated were sorted based on tdTomato expression in
721 comparison to BC-3 cells lacking the reporter. tdTomato was plotted against green fluorescence,
722 as autofluorescence is detected in the green channel. Gates indicated by red and cyan colors were
723 set for collecting tdTomato-positive and negative cells, respectively.
724
725 **Supplemental Figure 3. Lack of IFN signaling induction by TPA and caspase inhibitors in**
726 **uninfected B cells.** BJAB cells were treated with 20 ng/ml TPA and/or the pan-caspase inhibitor
727 IDN-6556 at 10 μM ("casp-i") for 48 hrs. BC-3 cells treated with TPA and IDN-6556 were used
728 as a positive control for induction of type I and III interferons. IFN-β (**A**) and IFN-λ1 (**B**) mRNA
729 levels were measured by qRT-PCR and normalized to 18S rRNA. Their levels are plotted

730 normalized to TPA and IDN-6556-treated BC-3 sample. n=4. **C.** Protein lysates were probed
731 with antibodies against phosphorylated IRF3 (Ser386), total IRF3, phosphorylated TBK1
732 (Ser172), total TBK1, ATF2, c-Jun, total RelA, phosphorylated RelA (Ser536), and β-actin as
733 loading control. Images shown are representative of 3 replicates.

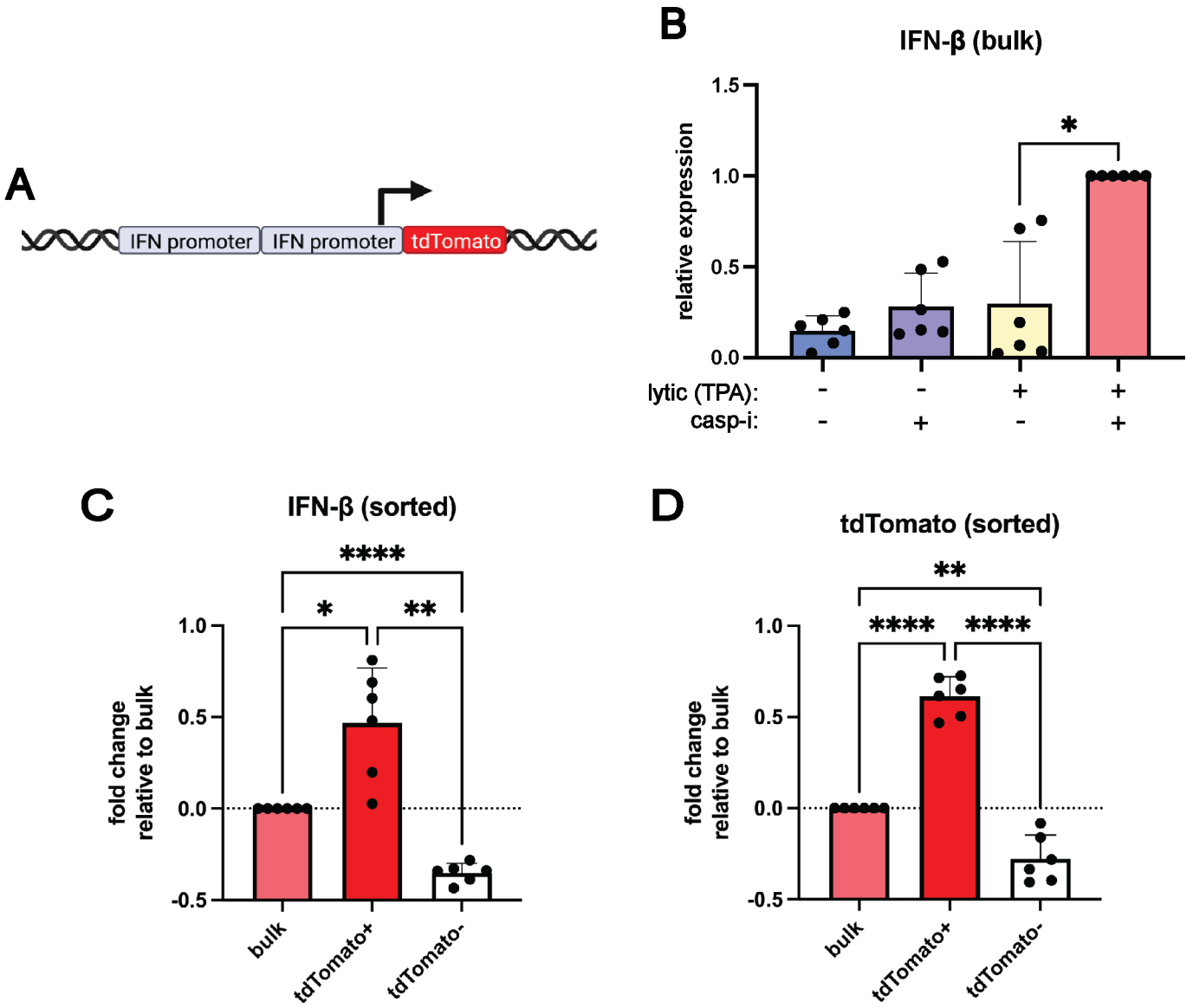

Figure 1. An IFN-β-promoter driven fluorescent reporter allows isolation of cells expressing high and low levels of IFN-β. A. Diagram of the IFN-βp-tdTomato reporter. Two copies of the 303 bp minimal promoter sequence for the human IFNB1 gene were cloned in front of the tdTomato fluorophore. This cassette was then introduced in BC-3 cells via lentiviral transduction leading to stable integration. **B-D.** BC3-IFN-βp-tdTomato reporter cells were treated with 20 ng/mL TPA for 48 hours to induce the lytic cycle ("lytic (TPA)") . Where indicated, the cells were also treated with the pan-caspase inhibitor IDN-6556 at 10 µM ("casp-i"). IFN-β and tdTomato mRNA levels were measured by RT-qPCR and normalized to 18S rRNA. For **B**, IFN-β mRNA levels are plotted normalized to the lytic+casp-i sample . For **C and D** the lytic+casp-i treated samples were sorted based on tdTomato expression and the fold enrichment in IFN-β and tdTomato RNA levels compared to unsorted ("bulk") samples is plotted in log10 scale. n=6.

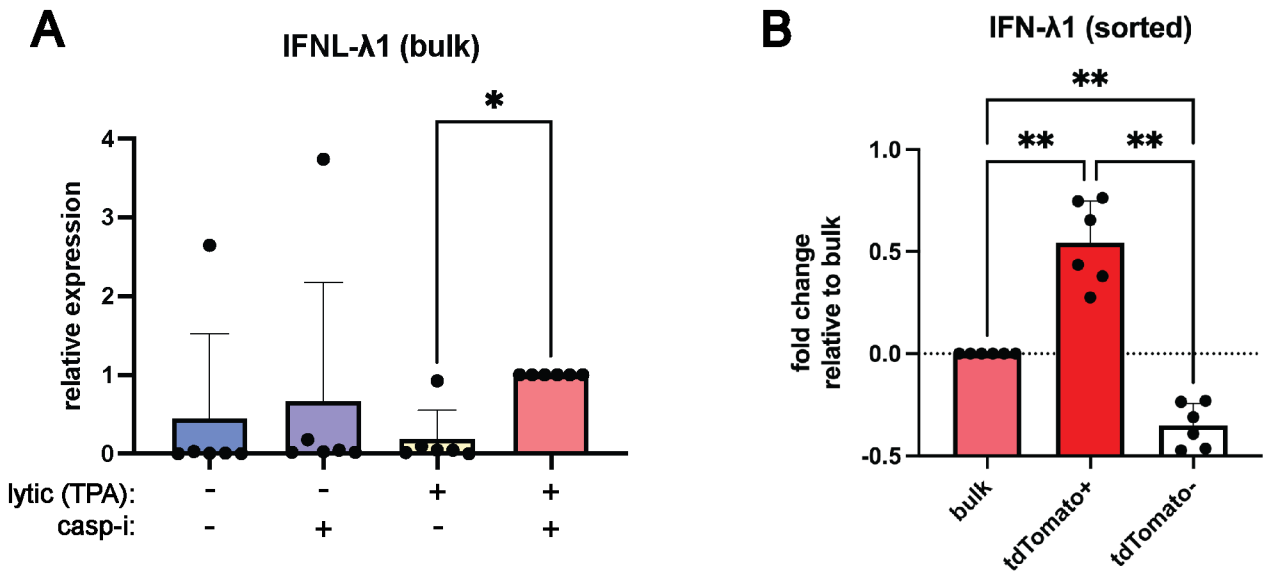

Figure 2. IFN-λ1 is expressed in the same set of cells that produce high levels of IFN-β, pointing to heterogeneity in the induction pathway rather than -stochastic IFN-β promoter firing. A. BC3-IFN-βp-tdTomato reporter cells were treated with 20 ng/ml TPA for 48 hours to induce the lytic cycle ("lytic (TPA)"). Where indicated, the cells were also treated with the pan-caspase inhibitor IDN-6556 at 10 μM ("casp-i"). IFN-λ1 mRNA was measured by RT-qPCR and normalized to 18S rRNA. For **A**, IFN-λ1 mRNA levels are plotted normalized to the lytic+casp-i sample. In **B**, the lytic+casp-i treated samples were sorted based on tdTomato expression and the fold enrichment in IFN-λ1 RNA levels compared to unsorted ("bulk") samples is plotted in log10 scale. n=6.

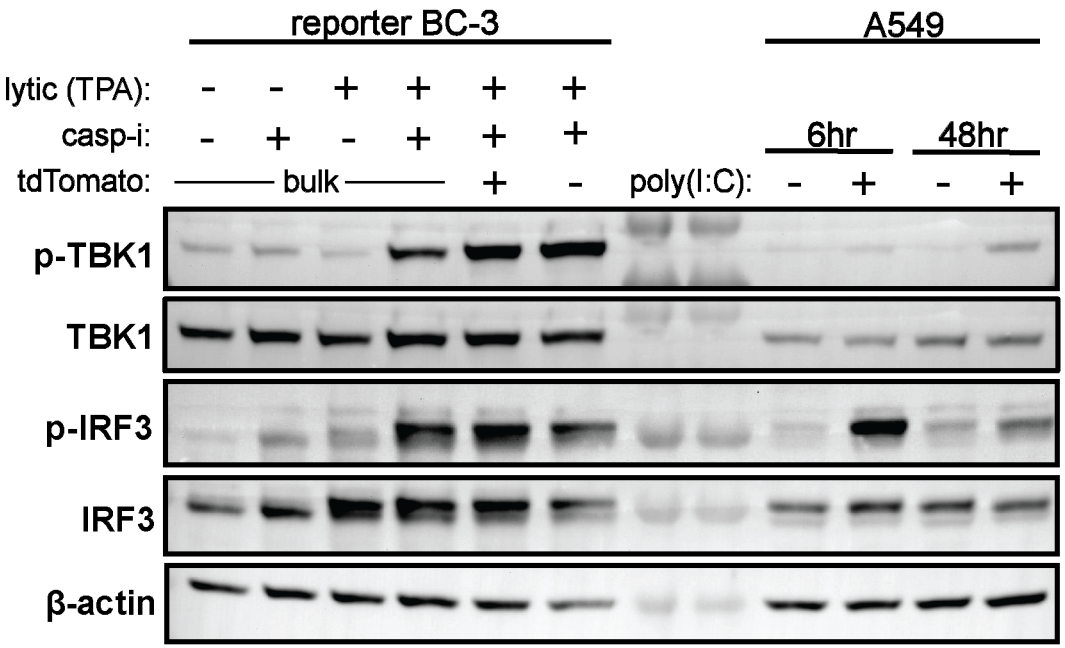

Figure 3. TBK1 and IRF3 are activated even in cells that do not transcribe IFN-β. BC3-IFN-βp-tdTomato reporter cells were treated with 20 ng/ml TPA for 48 hours to induce the lytic cycle ("lytic (TPA)"). Where indicated, the cells were also treated with the pan-caspase inhibitor IDN-6556 at 10 μM ("casp-i"). Protein was isolated from treated cells without sorting ("bulk"), or, for the lytic+casp-i treated sample, after sorting based on tdTomato expression. Protein lysates were probed for phosphorylated IRF3 (Ser386), total IRF3, phosphorylated TBK1 (Ser172), total TBK1, and β-actin as a loading control. As a positive control for IRF3 and TBK1 activation/ phosphorylation, A549 cells were treated with poly(I:C) for 6 and 48 hours before protein lysates were collected. Images shown are representative of 3 replicates.

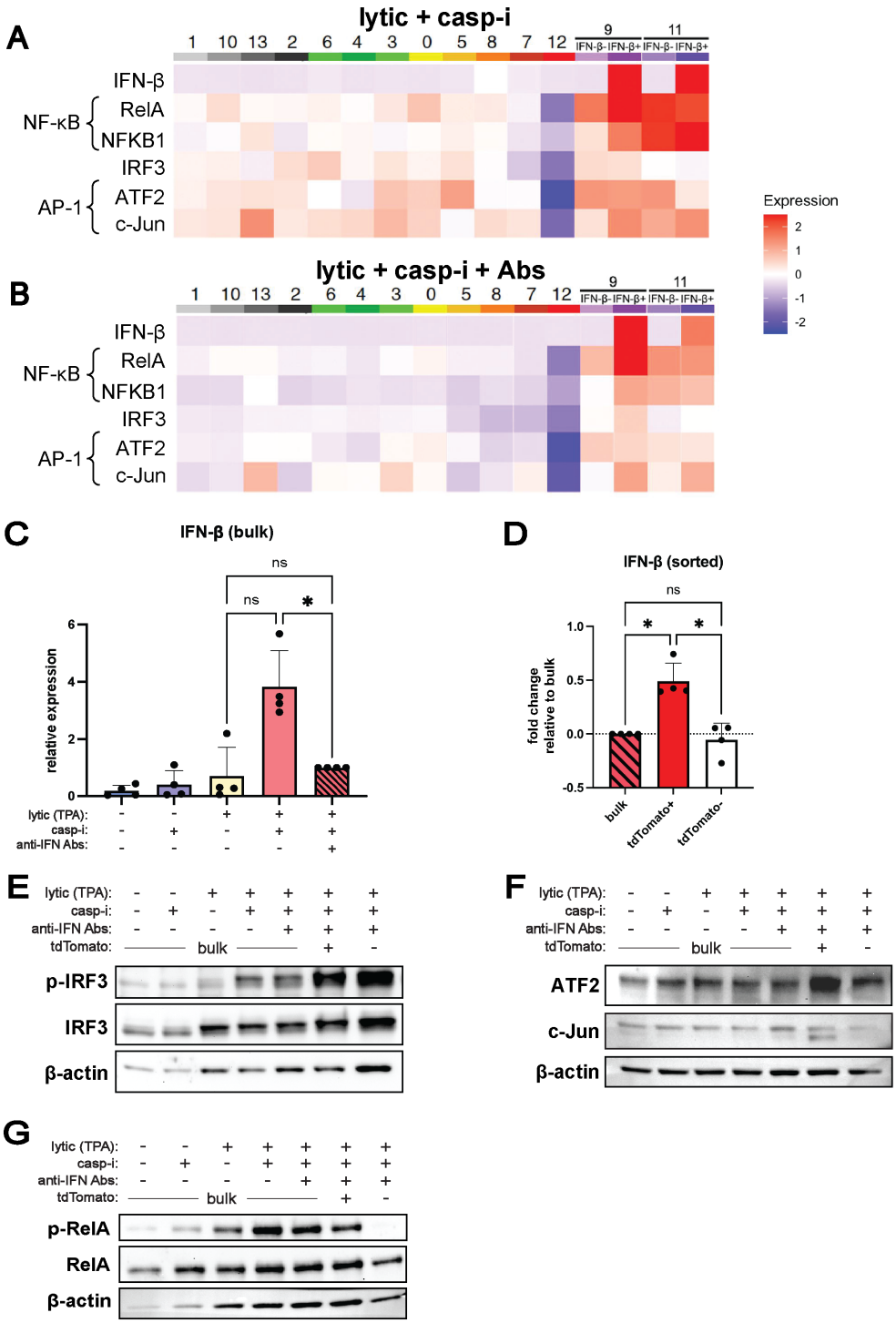

Figure 4. Levels of the AP-1 subunit ATF2 and phosphorylation of the NF-κB subunit RelA are higher in IFN-β high cells. A-B. Re-analysis of single cell RNA sequencing (scRNA-seq) data in Tabtieng, Lent et al 2022. iSLK.219 cells were treated with 1 µg/mL doxycycline for 4 days to induce the lytic cycle ("lytic"). The cells were also treated with the pan-caspase inhibitor IDN-6556 at 10 µM ("casp-i"), as well as a mixture of antibodies against type I interferon and its receptor ("anti-IFN Abs") (**B** only) to block IFN-β paracrine signaling where indicated. Average mRNA levels of genes in the IFN-β enhanceosome from the scRNA-seq data are shown for each of the 12 clusters of cells identified by the original analysis. The IFN-β-positive clusters 9 and 11 were further separated into two groups based on the IFN-β status of individual cells. **C-G.** BC3-IFN-βp-tdTomato reporter cells were treated with 20 ng/ml TPA for 48 hours to induce the lytic cycle ("lytic (TPA)"). Where indicated, the cells were also treated with the pan-caspase inhibitor IDN-6556 at 10 µM ("casp-i") and with a mixture of antibodies against type I interferon and its receptor ("anti-IFN Abs") to block IFN-β paracrine signaling. The lytic+casp-i+anti-IFN Abs treated samples were also sorted based on tdTomato expression in D-G. **C-D.** IFN-β RNA was measured by RT-qPCR and normalized to 18S rRNA. In C, IFN-β RNA levels are plotted normalized to the lytic+casp-i sample. In D, the fold enrichment in IFN-β RNA levels is compared to unsorted ("bulk") samples plotted in log10 scale. n=4. **E-G.** Western blots of protein samples from unsorted ("bulk") and sorted cells. Protein lysates were probed for: (**E**) phosphorylated IRF3 (Ser386), total IRF3, (**F**) ATF2, c-Jun, (**G**) phosphorylated RelA (Ser536), total RelA, β-actin was used as loading control. Images shown are representative of 3 replicates.

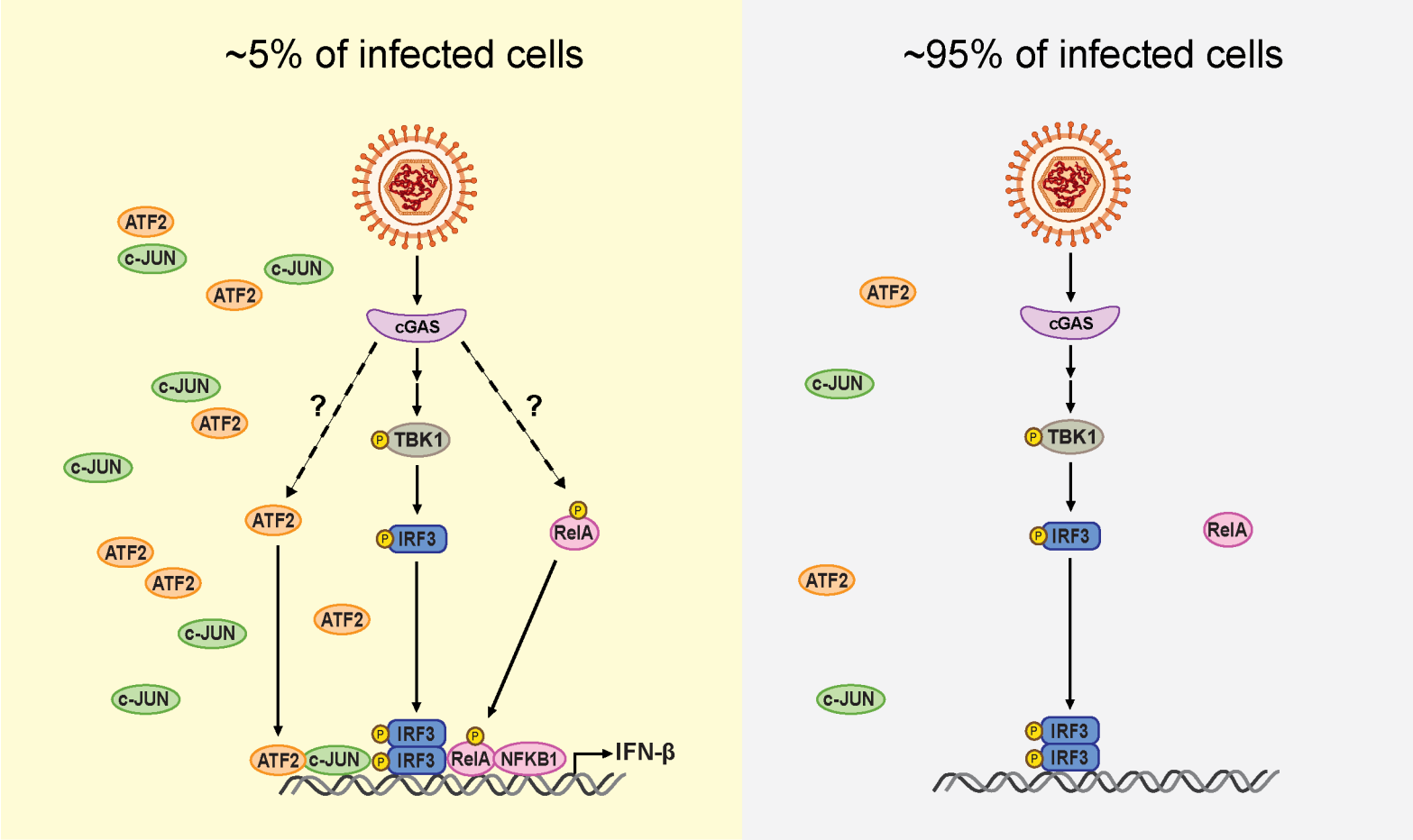

Figure 5. Model of regulation of heterogeneous IFN-β expression by components of the IFN-β enhanceosome. (Left) In the rare cells that induce IFN-β during viral infection, there are high levels of the AP-1 factor ATF2 and the NF-κB subunit RelA becomes phosphorylated in addition to IRF3 in response to infection. This results in the formation of the IFN-β enhanceosome and IFN-β transcription. (Right) In the majority of virally infected cells, there are lower amounts of ATF2, and RelA is not phosphorylated during infection. While IRF3 is still activated, the full IFN-β enhanceosome does not form and IFN-β is not induced.

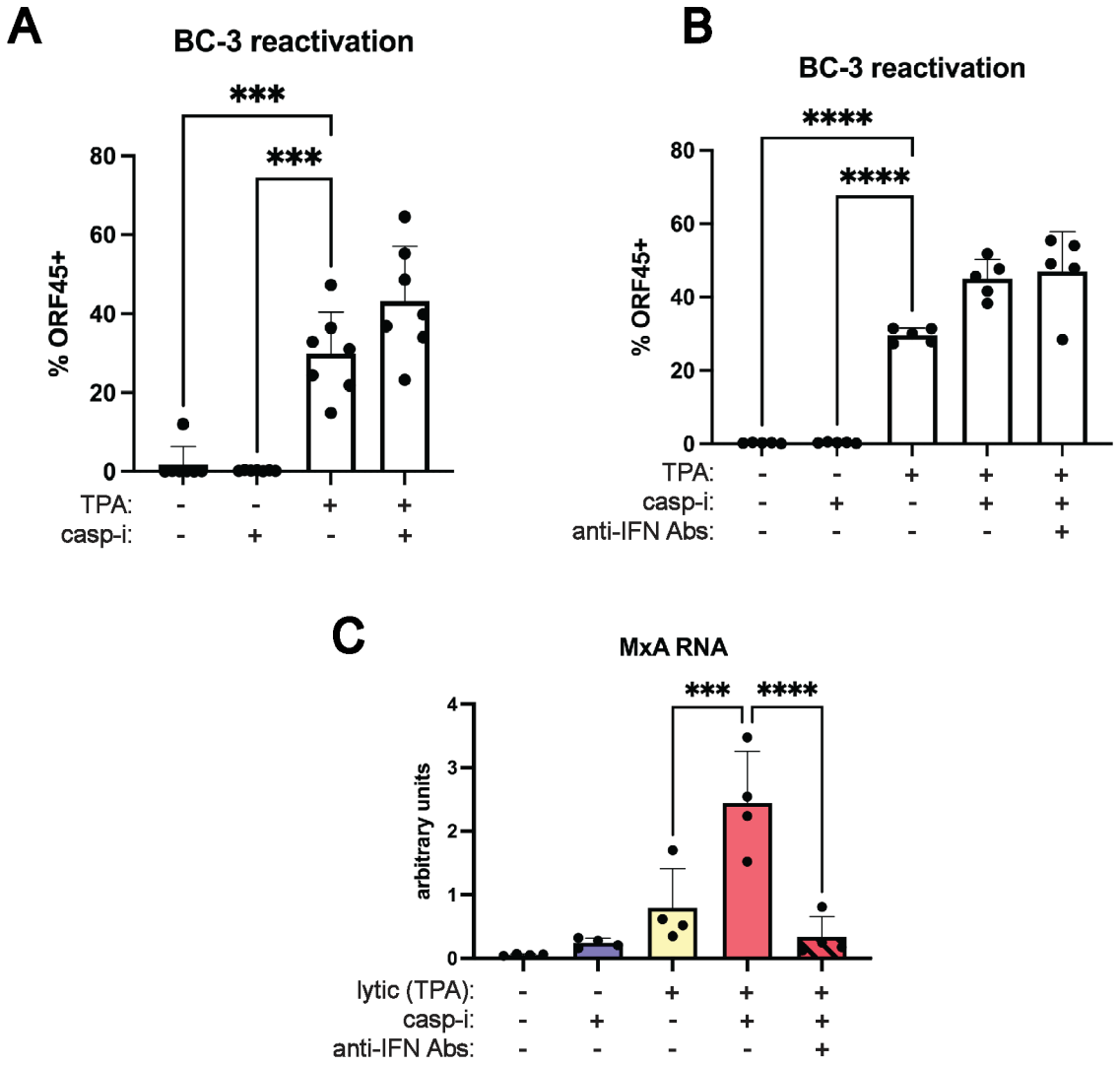

Supplemental Figure 1. Controls showing efficient reactivation of BC3-IFN-βp-tdTomato and efficient block of interferon stimulate gene induction by anti-IFN antibodies. BC3-IFN-βp-tdTomato reporter cells were treated with 20 ng/ml TPA for 48 hours to induce the lytic cycle ("lytic"). Where indicated, the cells were also treated with the pan-caspase inhibitor IDN-6556 at 10 µM ("casp-i") and in **B and C** a mixture of antibodies against type I interferon and its receptor ("anti-IFN Abs") to block IFN-β paracrine signaling. The percentage of cells expressing the lytic KSHV protein ORF45 was measured by flow cytometry. Graphs A and B show the reactivation rates for all BC3 experiments shown (**A**) n=7, (**B**) n=5. **C.** mRNA levels of MxA, an interferon stimulated gene (ISG) were measured by qRT-PCR and normalized to 18S rRNA. n=4.

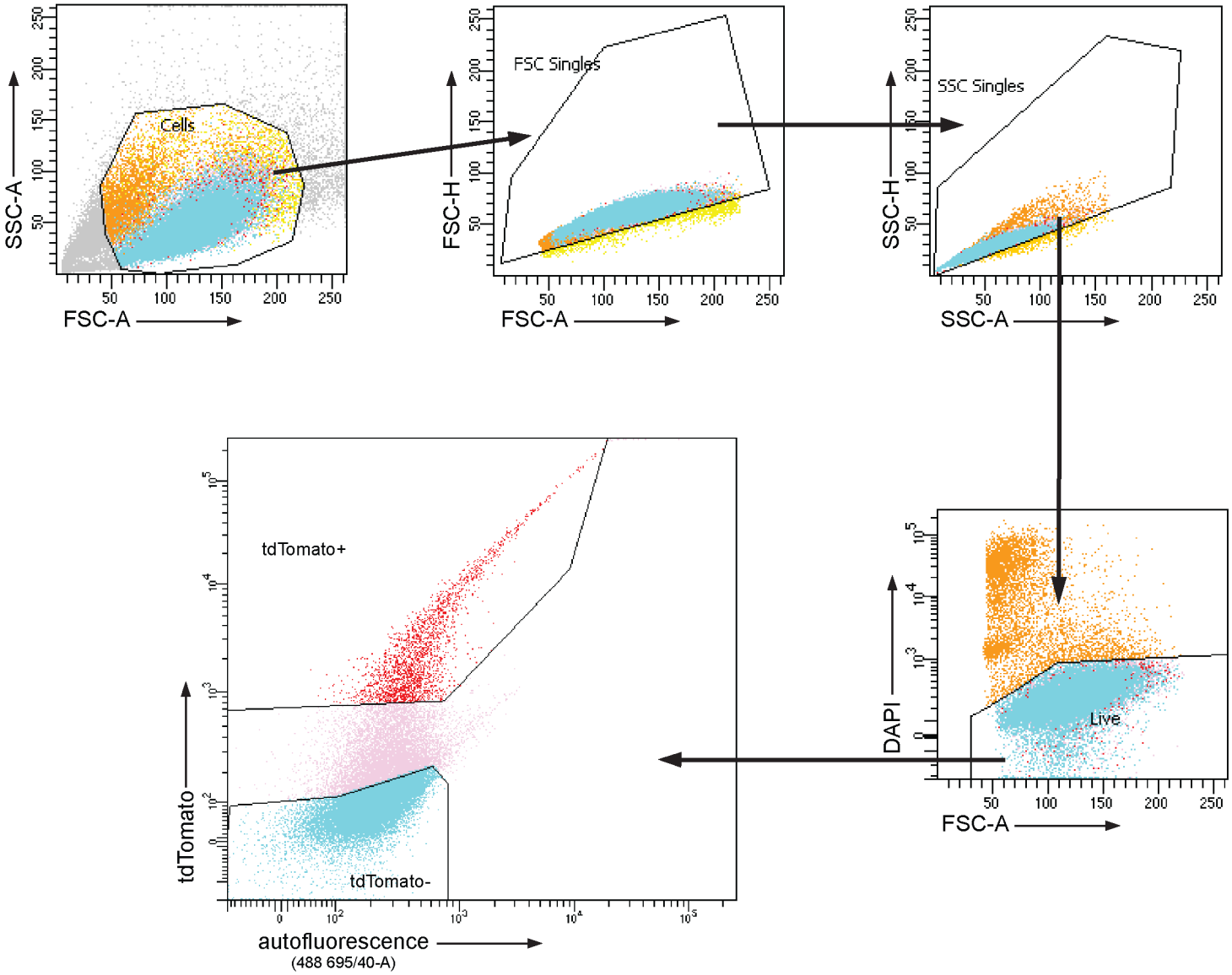

Supplemental Figure 2. Representative gating strategy for FACS. Plots showing an example gating for BC3-IFN-βp-tdTomato cell sorting based on tdTomato fluorescence. Gates for tdTomato-positive and negative populations were drawn conservatively to prevent false positives and negatives. In this particular experiment, BC3-IFN-βp-tdTomato reporter cells were treated with 20 ng/ml TPA and 10 μM IDN-6556 (IDN) for 48 hours to induce the lytic cycle and trigger IFN-β expression and tdTomato production. Side scatter (SSC) and forward scatter (FSC) area (A) and height (H) were used to separate cells from debris and remove doublets. DAPI staining was used to identify live cells. Cells thus gated were sorted based on tdTomato expression in comparison to BC-3 cells lacking the reporter. tdTomato was plotted against green fluorescence, as autofluorescence is detected in the green channel. Gates indicated by red and cyan colors were set for collecting tdTomato-positive and negative cells, respectively.

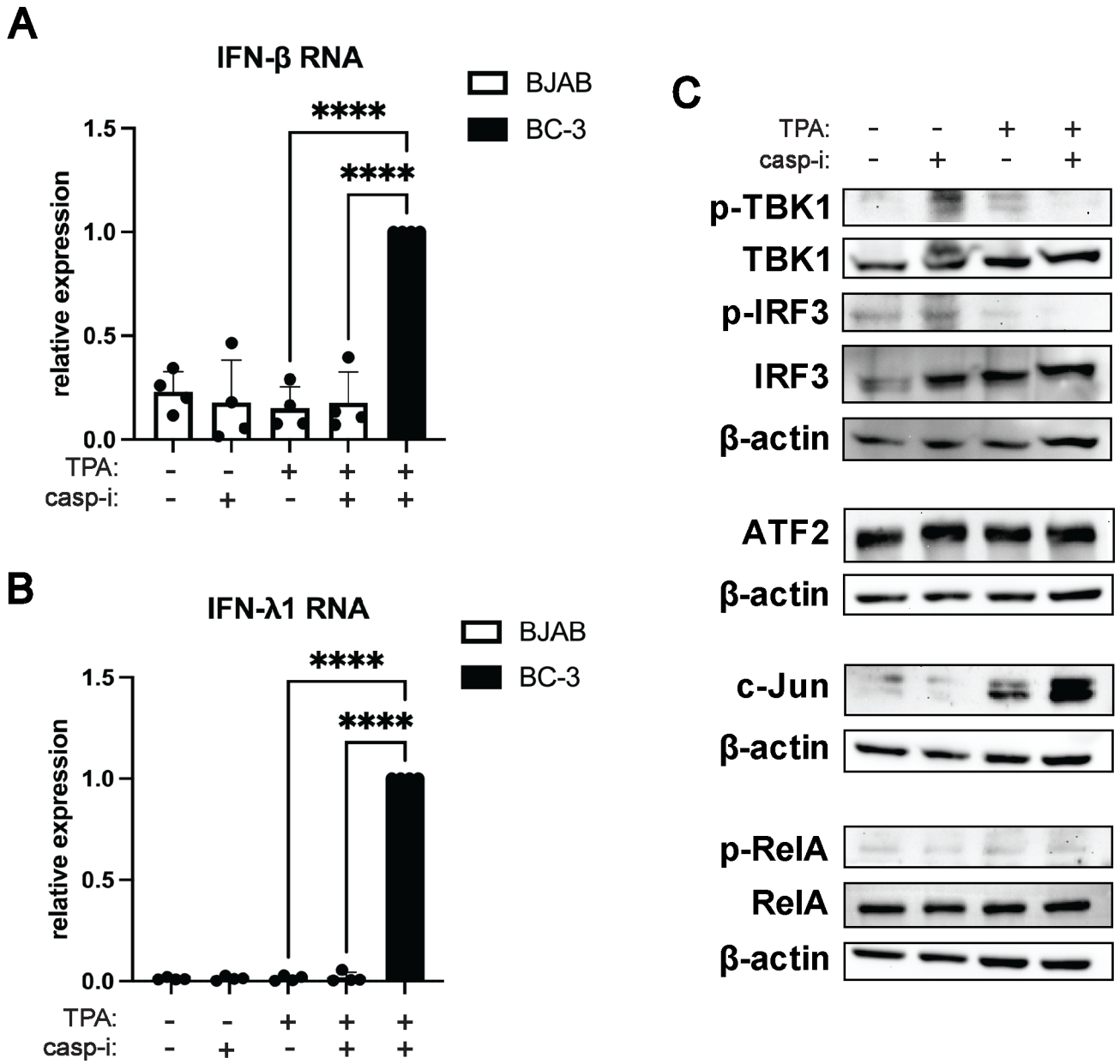

Supplemental Figure 3. Lack of IFN signaling induction by TPA and caspase inhibitors in uninfected B cells. BJAB cells were treated with 20 ng/ml TPA and/or the pan-caspase inhibitor IDN-6556 at 10 μM ("casp-i") for 48 hrs. BC-3 cells treated with TPA and IDN-6556 were used as a positive control for induction of type I and III interferons. IFN-β (**A**) and IFN-λ1 (**B**) mRNA levels were measured by qRT-PCR and normalized to 18S rRNA. Their levels are plotted normalized to TPA and IDN-6556-treated BC-3 sample. n=4. **C.** Protein lysates were probed with antibodies against phosphorylated IRF3 (Ser386), total IRF3, phosphorylated TBK1 (Ser172), total TBK1, ATF2, c-Jun, total RelA, phosphorylated RelA (Ser536), and β-actin as loading control. Images shown are representative of 3 replicates.